Tremella fuciformis polysaccharide: enhancing ischemic hypoxic adaptation of mesenchymal stem cells

Lei Yang,* Shan Chen,* Gang Zhao, Wei Gou, Weiwei Wang, Zhipeng Hu

Department of Vascular Surgery, General Hospital of Ningxia Medical University, Yinchuan, China.
**These authors contributed equally to this work as the co-first author.*

Abstract

Human Placenta-Derived Mesenchymal Stem Cells (HP-MSCs) are recognized for their potential in treating various diseases due to their multidirectional differentiation and immunomodulatory abilities. However, the therapeutic efficacy is often compromised in ischemic and hypoxic environments. *Tremella Fuciformis* Polysaccharide (TFP), a natural polysaccharide known for its immunomodulatory and anti-inflammatory properties, stands a good chance of overcoming this limitation. Our study investigates whether TFP enhances the therapeutic efficacy of HP-MSCs under ischemic-hypoxic conditions by inhibiting autophagy, with a focus on the role of the ERK signaling pathway. HP-MSCs were cultured under hypoxic conditions to simulate an ischemic environment and TFP was added to investigate its effects on MSC bioactivity, apoptosis, and proliferation. Mechanistic studies were conducted to assess the activation of the ERK signaling pathway and the expression of autophagy-related markers. TFP enhanced HP-MSC bioactivity under hypoxia by reducing apoptosis and promoting proliferation. Mechanistic analysis revealed that TFP enhanced the ability of HP-MSCs to adapt to hypoxic stress by activating the ERK signaling pathway. This activation led to the inhibition of autophagy-related markers, suggesting that TFP plays a protective role in hypoxia-induced cell stress. TFP enhances the therapeutic potential of HP-MSCs in ischemic-hypoxic conditions by inhibiting autophagy through ERK signaling pathway activation. These findings provide a theoretical foundation for the use of TFP in treating lower limb ischemia and highlight its potential to improve treatment protocols and outcomes.

Key Words: *Tremella fuciformis* polysaccharide, human placenta-derived mesenchymal stem cells, autophagy, ischemic and hypoxic, ERK.

Eur J Transl Myol 36 (1) 14289, 2026 doi: 10.4081/ejtm.2025.14289

Mesenchymal Stem Cells (MSCs) are pluripotent stem cells with self-renewal and multidirectional differentiation potential.[1] They are present in various tissues, including bone marrow, adipose tissue, the umbilical cord, and the placenta, and have been extensively studied for their roles in immune regulation, anti-inflammation, and tissue repair.[2]

As an important constituent in traditional Chinese medicine, Tremella Fuciformis Polysaccharide (TFP)[3] has attracted widespread attention because of its multiple biological activities. Owing to its immunomodulatory, anti-inflammatory, and antioxidant effects,[4,5] TFP has been used in traditional medicine to enhance immunity and nourish the body. It also shows significant therapeutic potential in modern medical research.[6]

Cellular autophagy is a critical physiological process that enables cells to respond to stress, such as nutrient deprivation, injury, and pathogen invasion, by degrading and recycling damaged or unwanted components.[7] Autophagy plays a crucial role in maintaining intracellular stability and is essential for cell survival, metabolic regulation, and antiaging.[8,9]

Focusing on the role of TFP in autophagy, this study investigated the role of TFP in HP-MSCs in the ischaemic-hypoxic microenvironment and further revealed that the ERK signaling pathway is a key regulator of TFP-regulated autophagy. These findings are expected to provide a basis for optimising human haematopoietic stem cell-based ischaemic hypoxia therapy.

Materials and Methods

Isolation and culture of HP-MSCs

Following the established method for HP-MSC isolation and culture at the Stem Cell Research Institute, Ningxia Medical University, 3–5 healthy full-term placentas were randomly selected. The acquisition of all human samples was approved by the Ethics Committee of General Hospital of Ningxia Medical University. Healthy full-term placentas were collected and transferred to a biosafety cabinet using sterile tools. The placentas were repeatedly rinsed with PBS (Servicebio) to remove blood and impurities. The placental tissue was minced into small pieces (1–2 mm^3) and incubated at 37°C, 5% CO2, and saturated humidity in Nuwacell ncMission hMSC serum-free medium containing 1×GlutaMAX™ and 50 μg/ml gentamicin. Once the cells migrated from the tissue mass, they were digested with TrypLE™ Express enzyme and isolated by sieving or centrifugation. The isolated cells were seeded at an appropriate density (1×10^6 cells/100 mm) in serum-free medium in Petri dishes (BIOFIL). The cells were collected for further passaging, and 3–5 passages were selected for experiments.

Identification of HP-MSCs

A total of 1×10^6 cells were harvested, and their surface antigens were analyzed via flow cytometry. After being harvested, the cells were washed with PBS, treated with trypsin or gently dissociated, centrifuged, and resuspended in flow cytometry staining buffer. Marker antibodies were then added, and the cells were incubated at 4°C for 30 minutes in the dark. After washing, at least 10,000 cells were analyzed via a BD FACS Aria flow cytometer with fluorescently labeled antibodies against CD73, CD90, CD105, CD14, CD34, CD45, and HLA-DR (BioLegend) to assess HP-MSC surface antigen expression.

Differentiation of HP-MSCs

HP-MSCs were seeded in osteogenic differentiation medium, and the medium was replaced every 3–4 days. After approximately 3 weeks of differentiation, Alizarin Red S staining was used to detect calcium deposition, Alcian blue staining was used for glycosaminoglycan deposition, and Oil Red O staining was used for lipid droplets to evaluate the potential of MSCs to differentiate into osteoblasts, chondrocytes, and adipocytes. The differentiation media and stains were purchased from Cyagen Biosciences.

Ischemic hypoxic microenvironment

HP-MSCs were plated at a density of 5×10^3 cells/cm^2 and cultured in complete DMEM until 80% confluence. The cells were treated with serum-free basal medium and incubated under 1% oxygen at 37°C and 5% CO2 for 6 hours.

Tremella fuciformis polysaccharide treatment

To prepare a 10 mg/mL stock solution, 12.5 g of *Tremella fuciformis* polysaccharide powder was dissolved in sterile phosphate buffered saline and was then subjected to 0.22 μm filter sterilization and preserved at -20°C until needed. Dilutions of the stock solution were made in culture medium to create the working concentration immediately before use. Unless specified all experiments were done with 100 μg/mL of TFP. For the cell proliferation assay (CCK-8 and EdU), TFP was added at the concentration of 100 μg/mL to the samples for the duration of the assay. For the apoptosis assays (Annexin V/PI staining and Western blot), cells were treated with 100 μg/mL for 24 hours before analysis. In the autophagy assays (mRFP-GFP-LC3B puncta imaging, Western blot), TFP was added at the the same concentration together with hypoxic exposure.

Western blot analysis

The cells were lysed in RIPA buffer (Servicebio) containing protease and phosphatase inhibitors (Servicebio). The protein concentration was determined via a BCA protein assay kit (Thermo). Proteins were separated via SDS–PAGE on a 10% polyacrylamide gel. The membrane was incubated overnight at 4°C with a primary antibody diluted in TBST containing 5% BSA. The membrane was incubated with an HRP-conjugated secondary antibody (Proteintech) for 1 hour at room temperature. The protein bands were detected via a chemiluminescent imaging system (Sizenberg Bio). Band intensity was quantified via ImageJ software and normalized to that of the β-Tubulin control.

Immunocytochemistry

Treated HP-MSCs were seeded on slides for cell crawling assays. Adherent or single cells were fixed with 4% paraformaldehyde at 4°C for 30 minutes. The membranes were then permeabilized in PBS containing 0.1% Triton X-100 (VETEC) for 15 minutes. Nonspecific binding was blocked with 0.01% PBST containing 10% goat serum for 30 minutes. The primary antibodies were diluted in antibody diluent and incubated overnight at 4°C. After washing, the samples were incubated with secondary antibodies (Proteintech) for 1 hour. The cells were then observed via a fluorescence microscope (OLYMPUS).

Cell proliferation assay

HP-MSCs treated under different conditions were seeded in 96-well plates (2×10^3 cells/well) for cell growth assays. CCK-8 (AbMole) was added to the wells, which were subsequently incubated at 37°C for 2 hours. The absorbance was then measured at 450 nm. EdU cell proliferation assays were conducted to assess cell proliferation. Approximately 1×10^5 cells were seeded in 12-well plates. After 24 hours, the cells were incubated with 500 μL of EdU reagent (KeyGEN BioTECH) per well for 2 hours. The membranes were permeabilized with 0.3% Triton X-100 for 15 minutes and then incubated with Click Reaction Reagent for 30 minutes at room temperature in the dark. Nuclei were counterstained with DAPI-containing mounting medium (Solarbio).

Cell apoptosis assay

Apoptosis rates were analyzed via an Annexin V-FITC Apoptosis Detection Kit (KeyGEN BioTECH). After treatment, the HP-MSCs were collected and resuspended in

binding buffer containing Annexin V-FITC and PI. The samples were then analyzed via a flow cytometer (Easy-Cell). BD FACSDiva 6.1.3 software (FlowJo-V10) was used to categorize cells into viable, necrotic, and apoptotic populations, followed by a comparison of apoptotic cell percentages across different groups.

Cell autophagy assay

The cells were infected in 24-well plates for 24 hours via an adenoviral vector expressing mRFP-GFP-LC3B (Hanbio Tech, Shanghai, China). Autophagic flux was assessed by counting GFP and mRFP puncta visible under a confocal microscope.

Statistical data

GraphPad Prism 5 and SPSS 17.0 were used for the statistical analyses. The data are expressed as the means ± standard errors from at least three independent experiments. The data from the experimental groups were compared via Student's t test. Multiple comparisons were conducted via ANOVA. Differences between groups were considered statistically significant at $p<0.05$.

Results

Phenotyping and differentiation of HP-MSCs

The morphology of HP-MSCs was uniformly spindle-shaped, as shown in Figure 1A. Flow cytometry is shown in Figure 1B, the cells highly expressed HP-MSC markers (CD73, CD90, and CD105) and exhibited minimal expression of markers for monocytes, macrophages, hematopoietic stem cells, leukocytes, and antigen-presenting cells (CD14, CD34, CD45, and HLA-DR). Figure 1C-E illustrates the trilineage differentiation of HP-MSCs into osteoblasts (alizarin red staining), chondrocytes (alcian blue), and adipocytes (oil red O staining) under specific induction conditions. These results confirmed that the cells exhibited typical MSC properties.

Proliferation and characterization of HP-MSCs in TFP

We performed EdU cell proliferation assay on cells from different treatment groups; DAPI staining (blue) was used to stain the nucleus, while EdU staining (green) was used to identify proliferating cells. The results were shown in Figure 2A and Figure 2B. TFP-treated cells proliferated significantly ($p<0.01$). Cell proliferation was also further assessed using the CCK-8 assay, and as shown in Figure 2C, the cell viability was significantly lower in the IHM group compared with the NC group ($p<0.05$), and significantly higher after TFP treatment ($p<0.01$).

Apoptosis of HP-MSCs in TFP

Apoptosis was assessed via Annexin V/PI double-staining flow cytometry, as shown in Figure 3A and 3B. The Q2 area represents late apoptotic cells, whereas the Q3 area represents early apoptotic cells. The proportions of cells in the Q2 and Q3 areas in the NC group were low (3.21% and 5.92%, respectively). Apoptosis significantly increased in the IHM group, while TFP treatment reduced both early and late apoptosis ($p<0.05$). The Western blot results are shown in Figure 3C and 3D. In the IHM group, the proapoptotic proteins Bax, C-Caspase-3, and C-PARP-1 were significantly upregulated, whereas the antiapoptotic protein Bcl-2 was significantly downregulated. In the IHM+TFP group, this pattern was reversed. Combined flow cytometry and western blotting results, the ischemic-hypoxic environment significantly promoted MSC apoptosis, as shown by increased apoptotic cell proportions, upregulated proapoptotic proteins (Bax, C-Caspase-3, and C-PARP-1), and downregulated antiapoptotic protein (Bcl-2) expression. Conversely, TFP partially attenuated the proapoptotic effects of ischemia and hypoxia on MSCs.

TFP inhibits autophagy in HP-MSCs

Figure 4A shows autophagic flux visualized by mCherry-eGFP-LC3B fluorescence, where the behavior of the GFP and mCherry signals reflects the autophagic flux. In the mCherry-eGFP-LC3B system, GFP fluorescence is quenched in acidic environments such as the lysosome, whereas mCherry maintains its fluorescence in both neutral and acidic conditions. Therefore, the presence of both green (GFP) and red (mCherry) signals (resulting in yellow colocalization) indicates that the autophagosome has not yet fused with the lysosome, suggesting that the autophagic flux is blocked. On the other hand, the presence of only red fluorescence (mCherry) without green fluorescence indicates that the autophagosome has successfully fused with the lysosome, representing active autophagic flux. In the NC group, mCherry (red) and GFP (green) signals show little overlap, indicating no significant autophagic flux activity. In the IHM group, the GFP signal is quenched due to its sensitivity to low pH in lysosomes, leaving mCherry as the dominant signal, indicating active autophagic flux. In the TFP group, yellow fluorescence is observed, representing the overlap of mCherry and GFP, indicating that the autophagosome has not fused with the lysosome, thus blocking autophagic flux. In the TFP+IHM group, more yellow fluorescence is seen, confirming that TFP blocks autophagic flux even in the presence of IHM stimulation. Quantification of LC3B puncta is shown in Fig 4B. The yellow bars represent autophagosomes, while the red bars represent autolysosomes. IHM significantly increases autolysosome formation, indicating increased autophagic flux. However, in the TFP+IHM group, autolysosome formation is reduced and autophagosome accumulation is increased, demonstrating that TFP blocks IHM-induced autophagic flux. LC3 and p62 are autophagy-related proteins; the conversion ratio of LC3 I to LC3 II serves as a marker of autophagic flux, while p62 is an autophagic substrate protein and its degradation level reflects autophagic flux. Figure 4C and 4D shows the western blot analysis and quantification of the autophagy-related proteins LC3 and p62. IHM decreases p62 levels and increases LC3-II expression, consistent with active autophagic flux. In contrast, the TFP+IHM group shows increased p62 accumulation and decreased LC3-II expression, indicating inhibition of autophagic flux.

Eur J Transl Myol 36 (1) 14289, 2026 doi: 10.4081/ejtm.2025.14289

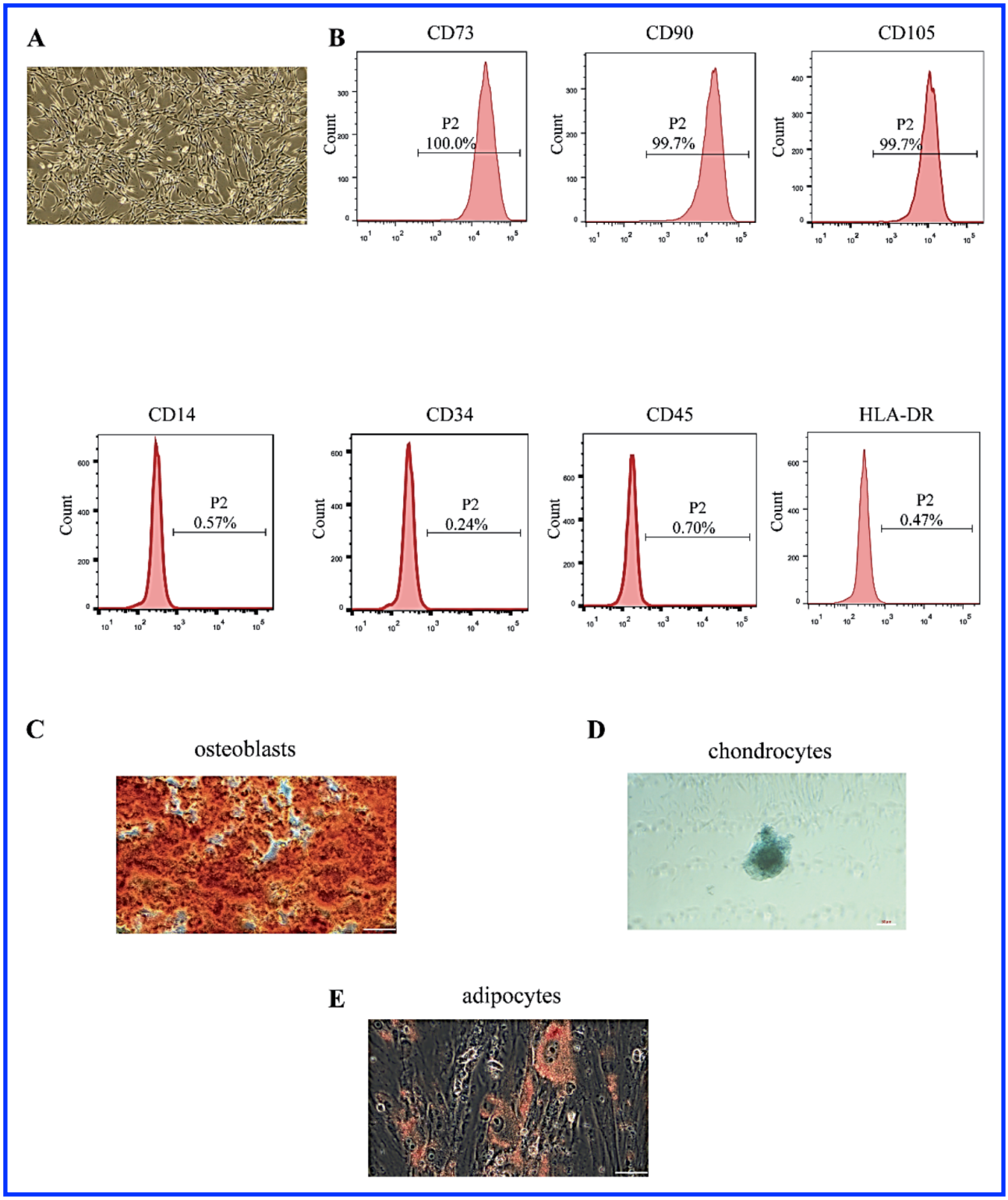

Figure 1. *Characterization of HP-MSCs. A) Morphology of cultured HP-MSCs; B) Flow cytometry showing high expression of MSC markers (CD73, CD90, CD105) and low expression of non-MSC markers (CD14, CD34, CD45, HLA-DR). Trilineage differentiation of HP-MSCs into C) osteoblasts, D) chondrocytes, and E) adipocytes. Scale Bars: (A), (C) 100μm; (D), (E) 50 μm. HP-MSCs, Human Placenta-Derived Mesenchymal Stem Cells.*

Eur J Transl Myol 36 (1) 14289, 2026 doi: 10.4081/ejtm.2025.14289

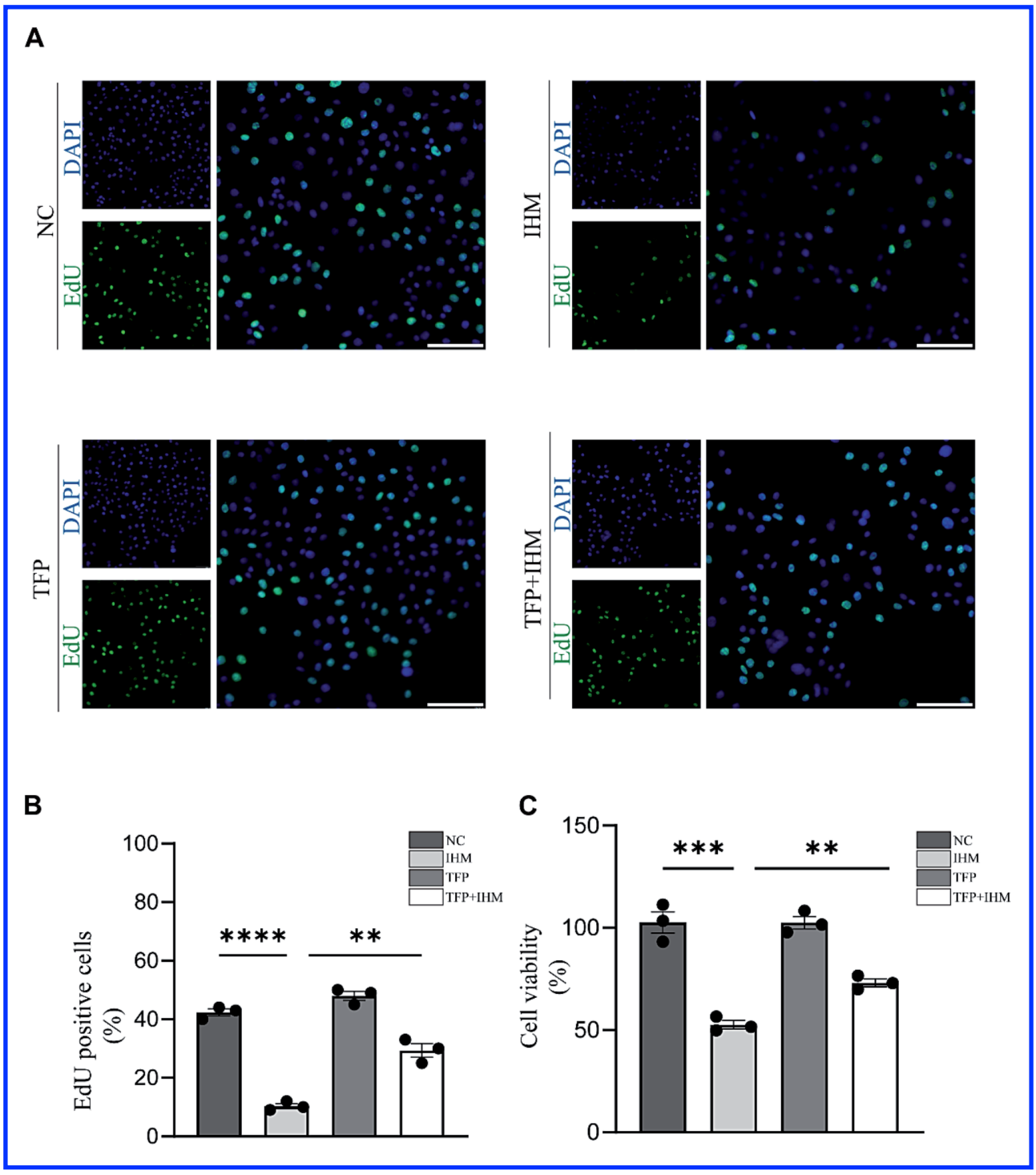

Figure 2. *Effects of TFP on HP-MSC Proliferation under IHM. A) EdU staining results, with DAPI (blue) marking nuclei and EdU (green) indicating proliferating cells. The green fluorescence signal EdU was significantly increased in the IHM+TFP group compared to the IHM group, implying that TFP promotes proliferation; B) Quantitative and intergroup difference analysis of green fluorescence signals in A; C) CCK-8 assay results showing reduced cell viability in the IHM group compared to NC, with partial restoration in the IHM+TFP group. The tests were carried out on three biological triplicates (n=3), and data are expressed as the mean–standard deviation. ****p<0.0001, ***p<0.001, **p<0.01. Scale Bars: (A),100μm, TFP, Tremella Fuciformis Polysaccharide; IHM, Ischemic Hypoxic Microenvironment; CCK-8, Cell Counting Kit-8; DAPI, 4',6-Diamidino-2-Phenylindole; EdU, 5-Ethynyl-2'-Deoxyuridine, all experiments were performed in triplicate (n=3). Data are mean±SD. Statistical significance was assessed by ANOVA.*

Eur J Transl Myol 36 (1) 14289, 2026 doi: 10.4081/ejtm.2025.14289

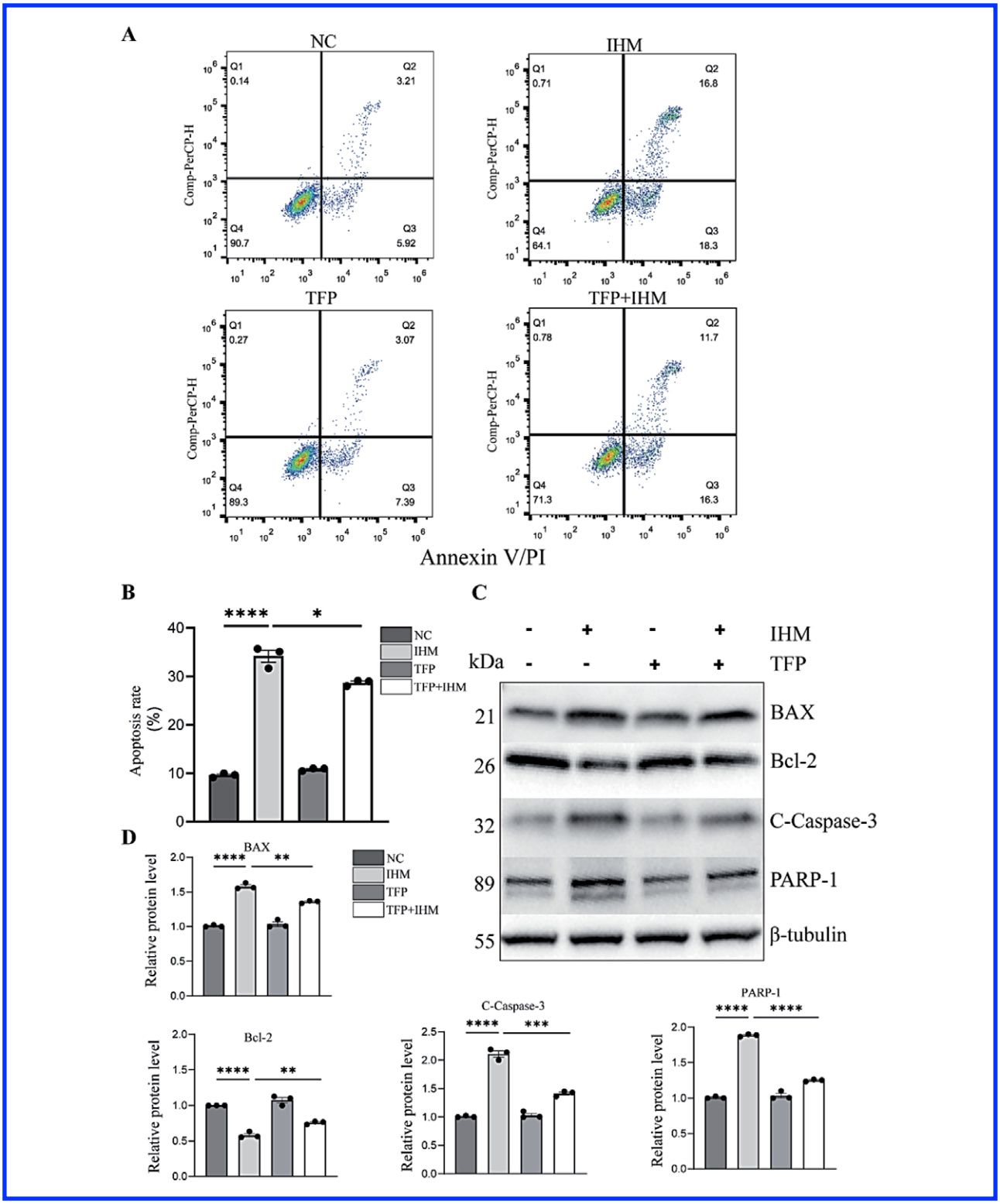

Figure 3. *TFP reduces apoptosis in HP-MSCs under hypoxia. A) Flow cytometry analysis using Annexin V/PI double staining, showing apoptosis distribution in different groups (Q1: Mechanically damaged cells, Q2: late apoptotic cells, Q3: early apoptotic cells, Q4: surviving cells); B) Quantitative data on apoptosis rates (early apoptosis and late apoptosis Q2+Q3) in different groups; C) and D) Western blotting and quantification of pro-apoptotic proteins (BAX, C-Caspase-3 and C-PARP-1) and anti-apoptotic protein Bcl-2 in HP-MSCs from different treatment groups. The tests were carried out on three biological triplicates (n=3), and data are expressed as the mean–standard deviation.* ****p<*0.0001*, ***p<*0.001*, **p<*0.01*, *p<*0.05*.

Eur J Transl Myol 36 (1) 14289, 2026 doi: 10.4081/ejtm.2025.14289

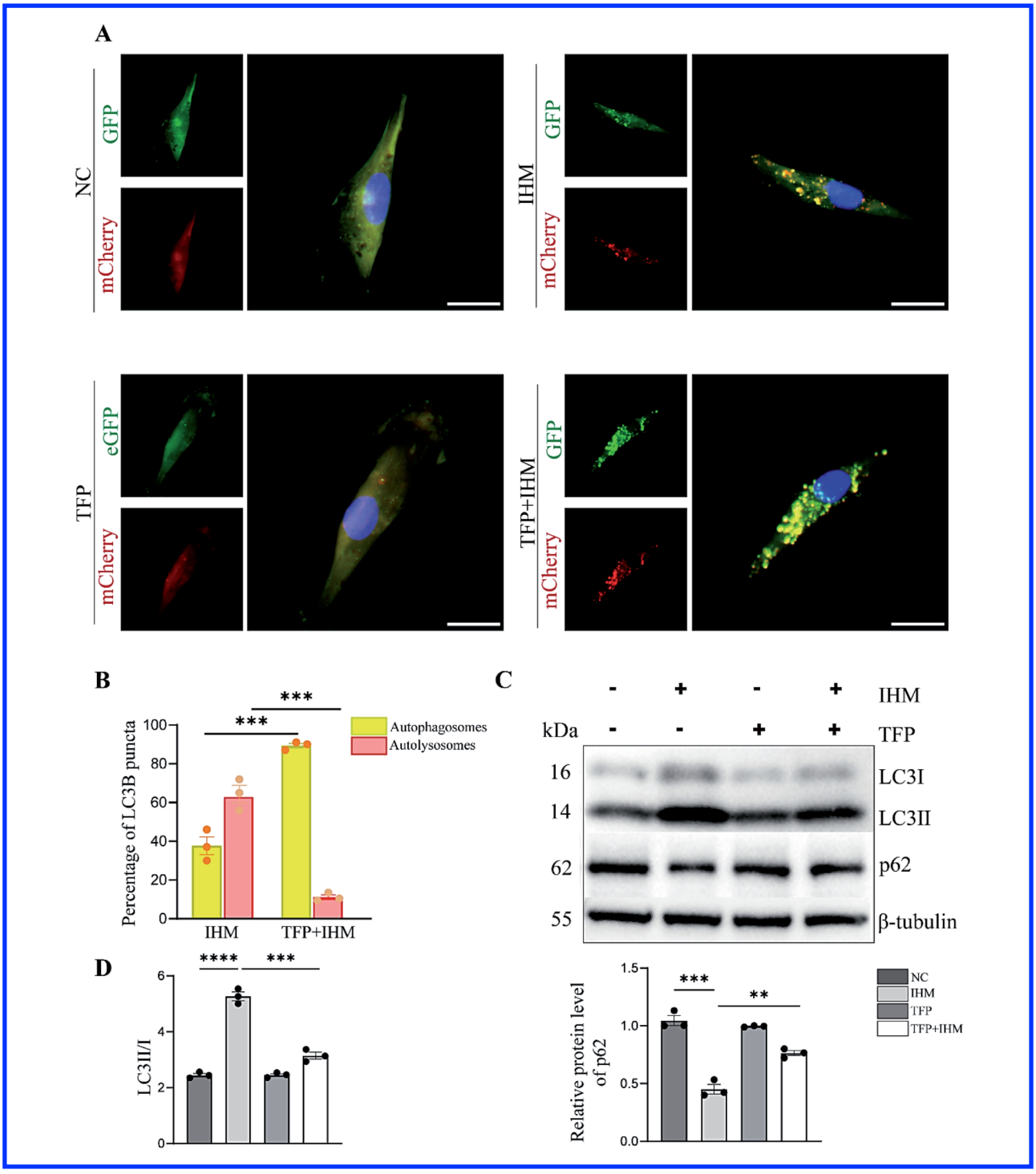

Figure 4. *TFP Inhibits Autophagy in HP-MSCs under IHM. A) mCherry-eGFP-LC3B dual fluorescence assay, NC group shows minimal fluorescence, the IHM group shows red fluorescence (mCherry) indicating autolysosome formation, the TFP group shows yellow fluorescence (GFP+mCherry) indicating autophagosome accumulation, the TFP+IHM group shows increased yellow fluorescence; B) Percentage of LC3B puncta. The IHM group shows a higher percentage of autolysosomes (red), whereas the TFP+IHM group shows a higher percentage of autophagosomes (yellow); C) Western blot for LC3 and p62. The IHM group shows higher levels of LC3-II and lower levels of p62, while the TFP+IHM group shows lower levels of LC3-II and higher levels of p62; D) Quantification of LC3-II/LC3-I ratio and p62. The tests were carried out on three biological triplicates (n=3), and data are expressed as the mean–standard deviation. ****p<0.0001, ***p<.001, **p<0.01. Scale Bars: (A),50μm.*

Verification TFP acts through autophagy

We evaluated the levels of autophagy-related proteins in HP-MSCs under ischemic–hypoxic conditions and used the autophagy inducer rapamycin (RAPA) to determine whether TFP exerts its effects through autophagy. The results of the Western blot analysis shown in Figure 5A revealed significant differences in the expression levels of the autophagy-related protein LC3 and the apoptosis markers C-Caspase-3 and C-PARP-1 across the different treatment groups. LC3 II expression was significantly increased in the IHM group. In the TFP+IHM group, LC3 II expression was significantly decreased. However, the addition of the autophagy inducer RAPA restored the LC3 II, C-Caspase-3, and C-PARP-1 levels. RAPA-induced autophagic flux reversed the inhibitory effect of TFP, supporting the hypothesis that TFP acts by inhibiting autophagic pathways.

TFP inhibits autophagy by activating the ERK signaling pathway

To explore how TFP reverses ischemia and hypoxia by inhibiting autophagy, we assessed ERK, p38, and JNK pathway protein expression levels in HP-MSCs. Figure 6A shows that p-ERK protein expression was increased in the IHM group, indicating that the ERK signaling pathway was activated under ischemic-hypoxic conditions. However, p-ERK protein expression was significantly lower in the TFP+IHM group than in the IHM group. To further verify the specific mechanism of the ERK signaling pathway, we added the ERK1/2 agonist Ro 67-7476 and observed its effects on autophagy and apoptosis markers. Figure 5B shows that Ro67-7476 significantly elevated p-ERK protein levels and reversed the inhibitory effect of TFP on LC3 II and p62 under ischemic-hypoxic conditions. Additionally, Ro 67-7476 reversed the expression of C-Caspase-3 and C-PARP-1, further confirming the critical role of the ERK signaling pathway in the regulation of autophagy and apoptosis by TFP.

Discussion

MSCs are widely applicable in disease treatments because of their multidirectional differentiation potential and robust regenerative capacity.[10] Recent studies have optimised the effects of MSCs by enhancing their activity and function through genetic modification, chemical pre-treatment and three-dimensional culture.[11] Additionally, the synergistic effects of MSCs with other cell types and biomaterials have been explored for more efficient and precise therapies.[12] However, the ischemic-hypoxic environment critically impacts the survival and function of these cells. This study revealed that TFP enhances the adaptive capacity of HP-MSCs under ischemic–hypoxic conditions by inhibiting autophagy.

Chinese medicine is widely recognized in modern medicine for its holistic approach, evidence-based treatments, natural therapies, and low toxicity. It has shown unique efficacy, particularly in chronic diseases.[13] Aside from its historical application in traditional medicine, TFP has also attracted increased attention in contemporary research for its immunomodulatory and anti-inflammatory properties. We add to this understanding by showing its further role in modulating autophagy in HP-MSCs under ischemic-hypoxic conditions.

Immunomodulation, and anti-inflammation. Studies indicate that TFP can inhibit tumor cell proliferation and migration by regulating immune cell function and antioxidant mechanisms, positively impacting cancer adjuvant therapy.[14,15] TFP has been shown to delay cellular aging in antiaging research.[16] These findings expand the applications of TFP and offer new insights and foundations for integrating Chinese medicine into modern medical practices. Our study demonstrated that TFP-treated MSCs in an ischemic–hypoxic microenvironment exhibited significantly increased proliferation and reduced apoptosis, enhancing their adaptation to the environment.

Autophagy is crucial for regulating cell survival, lymphocyte homeostasis, and cytokine production.[17] Under pathological conditions, autophagy removes damaged organelles and proteins, maintaining cellular homeostasis.[18] The benefits of autophagy include removing damaged organelles and proteins, reducing the accumulation of harmful substances, promoting cell renewal, and maintaining cellular health.[19,20] However, excessive autophagy can lead to cell death, particularly in hypoxic environments.[21] In the treatment of lower limb ischemia, autophagy is closely tied to cell survival, tolerance, tissue repair, and regeneration.[22,23] Our study demonstrated that TFP reduces cell death under ischemic–hypoxic conditions by inhibiting autophagy, thereby increasing MSC survival and function.

The ERK signaling pathway plays a crucial role in regulating cellular autophagy and maintaining metabolic homeostasis.[24,25] It plays a crucial role in cell proliferation, differentiation, and survival.[26] The ERK signaling pathway is also crucial in vascular remodeling pathology.[27] It mediates angiogenesis by regulating cellular activity and the expression of angiogenic factors. Some studies prove that the ERK signaling pathway regulates angiogenesis, improving local microcirculation and restoring the blood supply to ischemic areas, thus alleviating ischemic disease progression.[28] In the present study, we found that TFP activated the ERK signaling pathway and significantly affected the autophagy of MSCs in the ischaemic-hypoxic environment, further enhancing their viability and proliferation.

We have demonstrated the role of TFP in regulating autophagy in HP-MSCs and its molecular mechanism in the ischaemic-hypoxic microenvironment. Lower limb ischaemia also occurs in an ischaemic-hypoxic environment, so we can combine TFP with MSCs for the treatment of lower limb ischaemia in future studies.

Every research work has some concerns and gaps. Firstly, all the experiments done were in vitro and in vivo studies are needed in order to investigate the therapeutic relevance of TFP in ischemic situations. Secondly, TFP involvement has been shown, but other pathways could also be involved and are for future research.

Conclusions

This study demonstrated that TFP inhibits autophagy, reduces apoptosis, promotes cell proliferation, and regulates HP-MSC viability under ischemic and hypoxic conditions by activating the ERK signalling pathway (Figure 7).

Eur J Transl Myol 36 (1) 14289, 2026 doi: 10.4081/ejtm.2025.14289

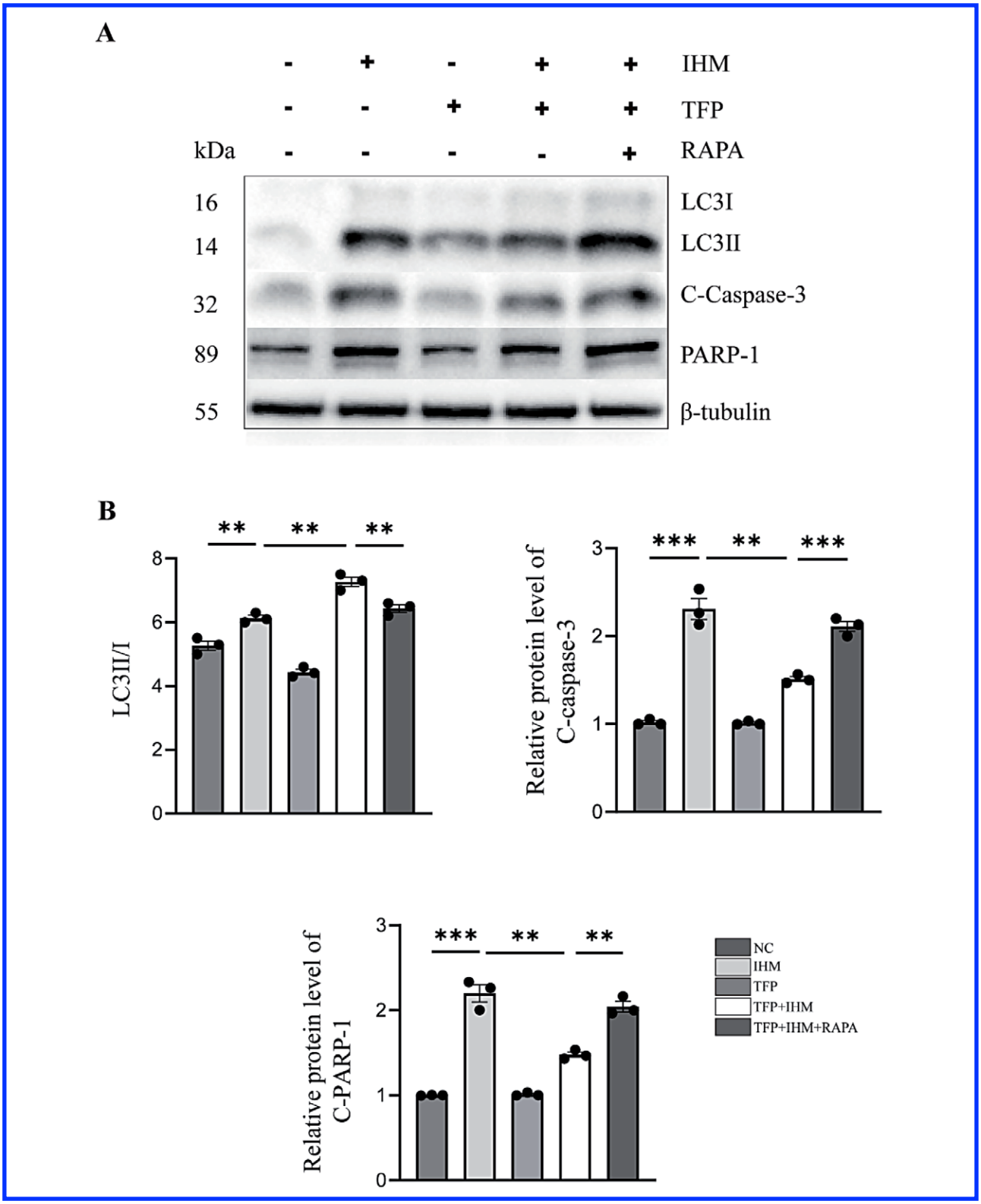

Figure 5. *TFP Inhibits Apoptosis by Modulating Autophagy in HP-MSCs. A) Western blot analysis of autophagy-related proteins LC3, C-caspase-3 and C-PARP-1 in different treatment groups and the effect of autophagy inducer RAPA on TFP-treated HP-MSCs under IHM (whether or not to reverse the activity of autophagy) to verify that TFP affects HP-MSCs under IHM through autophagy; B) Western blot quantification including relative protein expression of LC3II/I, C-caspase-3 and C-PARP-1. The tests were carried out on three biological triplicates (n=3), and data are expressed as the mean–standard deviation. ***p< 0.001, **p< 0.01. RAPA, Rapamycin.*

Eur J Transl Myol 36 (1) 14289, 2026 doi: 10.4081/ejtm.2025.14289

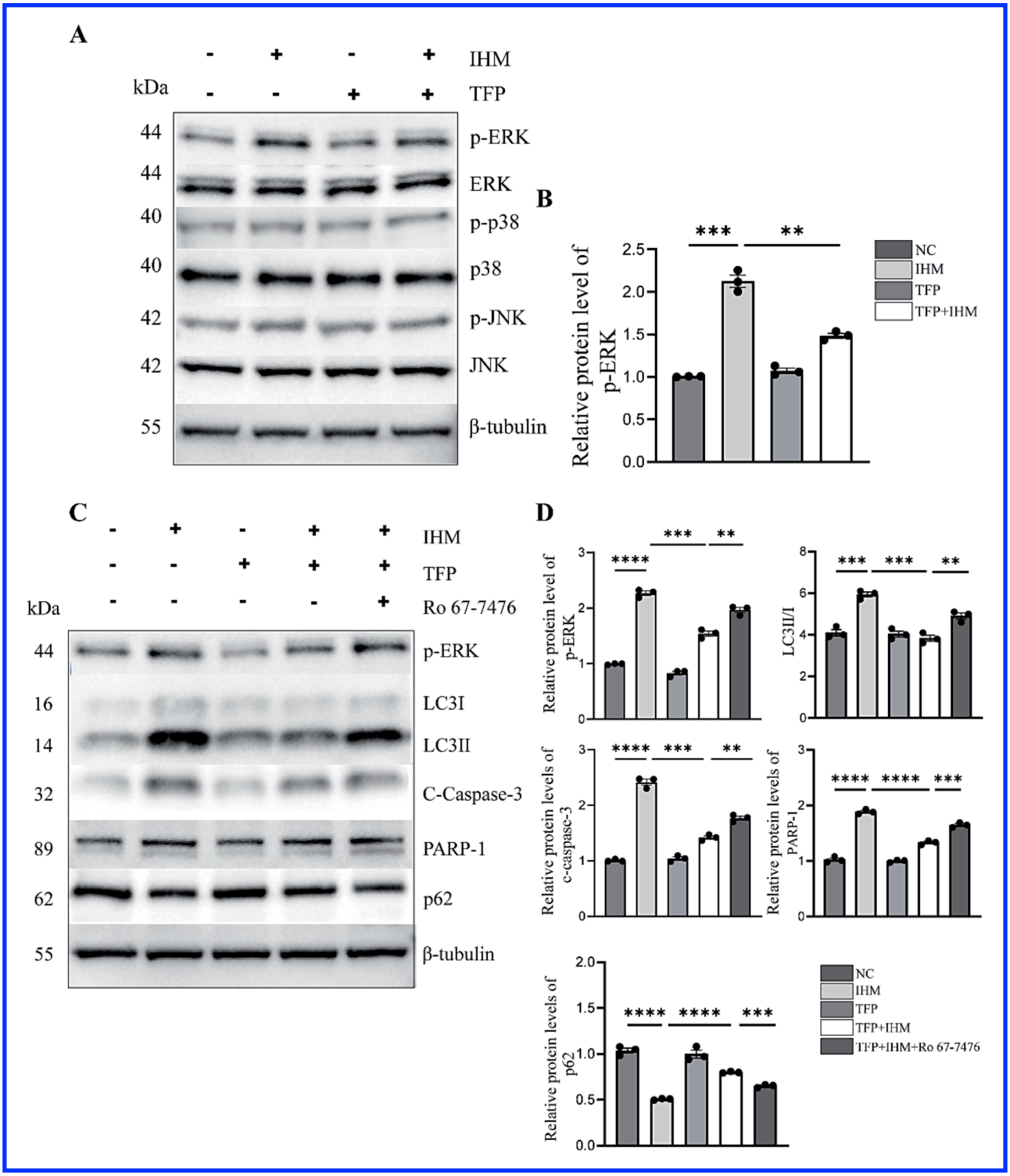

Figure 6. *TFP Inhibits Autophagy via the ERK Signaling Pathway in HP-MSCs. A) and B) Western blot analysis of ERK, p38 and JNK pathway proteins in HP-MSCs treated with or without TFP under ischemic hypoxic conditions and quantitative analysis. (C)-(D) Western blotting and quantitative analysis of the effects of the ERK agonist Ro 67-7476 on the expression of p-ERK, autophagy markers (LC3 II, p62), and apoptosis markers (C-Caspase-3, C-PARP-1), The tests were carried out on three biological triplicates (n=3), and data are expressed as the mean–standard deviation. ****p<0.0001, ***p<0.001, **p<0.01. Demonstrating the role of the ERK pathway in the regulation of autophagy and apoptosis by TFP. All experiments were performed in three independent biological replicates (n=3). Data are presented as mean±SD. Statistical significance was determined by one-way ANOVA.*

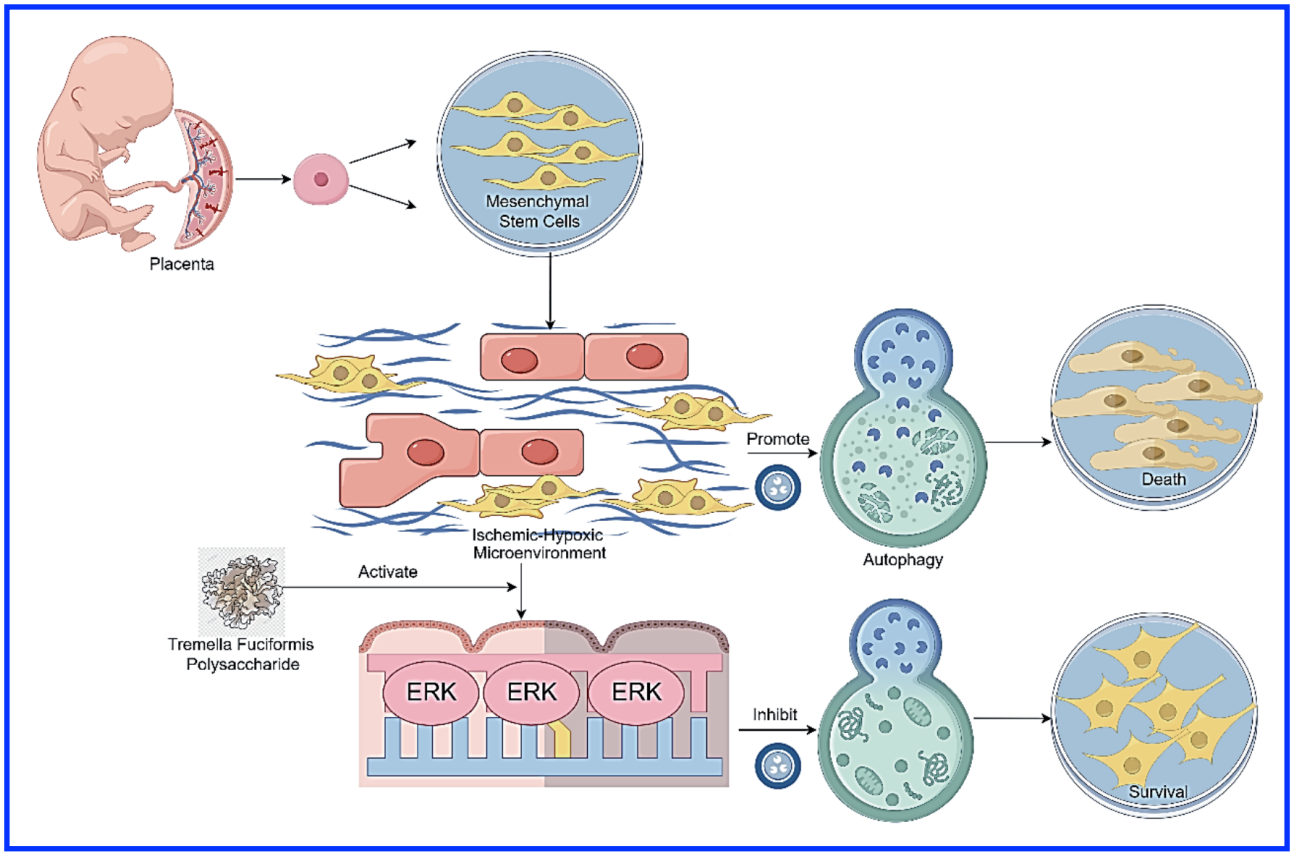

Figure 7. *Graphical abstract of the mechanism by which TFP enhances the therapeutic potential of HP-MSCs in ischaemia and hypoxia by inhibiting autophagy.*

Conflict of interest

The authors declare no conflict of interest, financial or otherwise.

Funding

This study was supported by the Natural Science Foundation of Ningxia Province, China (2022AAC03512, 2022AAC03527, 2024AAC03555).

Contributions

Zhipeng Hu, conceived and designed the study; Lei Yang, Shan Chen, performed the literature search and data extraction; Gang Zhao, Wei Gou analyzed the data; Lei Yang, Weiwei Wang, drafted the manuscript. All authors had access to the study data and had approved the final manuscript.

Ethical statement

Studies were performed in accordance with ethical principles based on the 1964 Declaration of Helsinki and its later amendments or comparable ethical standards, International Council for Harmonisation Guideline for Good Clinical Practice, and applicable laws and regulations. The human tissue collection involved in this experiment was approved by the Medical Ethics Review Committee of the General Hospital of Ningxia Medical University under the ethical number (KYLL-2021-797). Written informed consent was obtained from all participants.

Availability of data and materials

All data generated or analyzed during this study are included in this article. Further enquiries can be directed to the corresponding author.

Corresponding author

Zhipeng Hu, Department of Vascular Surgery, General Hospital of Ningxia Medical University, Yinchuan, China.
E-mail: hzp345397581@163.com
ORCID ID: 0009-0005-3927-058X

Co-author

Lei Yang
E-mail: yl435920214@163.com
ORCID ID: 0009-0006-8796-4583

Shan Chen
E-mail: 15008675478@163.com
ORCID ID: 0009-0002-5619-4994

Gang Zhao
E-mail: 18209616688@163.com
ORCID ID: 0009-0007-5541-4947

Wei Gou
E-mail: shini103@163.com
ORCID ID: 0009-0001-1400-8551

Weiwei Wang
E-mail: yww1830968707@163.com
ORCID not available

References

1. Han Y, Yang J, Fang J, et al. The secretion profile of mesenchymal stem cells and potential applications in treating human diseases. Signal Transduct Targeted Ther 2022;7:92.
2. Yang Y, Peng Y, Li Y, et al. Role of stem cell derivatives in inflammatory diseases. Front Immunol 2023; 14:1153901.
3. Ge X, Huang W, Xu X, et al. Production, structure, and bioactivity of polysaccharide isolated from *Tremella fuciformis* XY. Int J Biol Macromol 2020;148: 173-81.
4. Lee J, Ha SJ, Lee HJ, et al. Protective effect of *Tremella fuciformis* Berk extract on LPS-induced acute inflammation via inhibition of the NF-κB and MAPK pathways. Food Function 2016;7:3263-72.
5. Xie L, Yang K, Liang Y, et al. *Tremella fuciformis* polysaccharides alleviate induced atopic dermatitis in mice by regulating immune response and gut microbiota. Front Pharmacol 2022;13:944801.
6. Ma X, Yang M, He Y, et al. A review on the production, structure, bioactivities and applications of *Tremella* polysaccharides. Int J Immunopathol Pharmacol 2021;35:20587384211000541.
7. Schwartz LM. Autophagic cell death during development–ancient and mysterious. Front Cell Develop Biol 2021;9:656370.
8. Xu Y, Yang X. Autophagy and pluripotency: self-eating your way to eternal youth. Trends Cell Biol 2022; 32:868-82.
9. Debnath J, Gammoh N, Ryan KM. Autophagy and autophagy-related pathways in cancer. Nature Rev Molec Cell Biol 2023;24:560-75.
10. Łabędź-Masłowska A, Vergori L, Kędracka-Krok S, et al. Mesenchymal stem cell-derived extracellular vesicles exert pro-angiogenic and pro-lymphangiogenic effects in ischemic tissues by transferring various microRNAs and proteins including ITGa5 and NRP1. J Nanobiotechnol 2024;22:60.
11. Thanaskody K, Jusop AS, Tye GJ, et al. MSCs vs. iPSCs: Potential in therapeutic applications. Front Cell Develop Biol 2022;10:1005926.
12. Al Subayyil A, Basmaeil YS, Alenzi R, Khatlani T. Human Placental Mesenchymal Stem/Stromal cells (pMSCs) inhibit agonist-induced platelet functions reducing atherosclerosis and thrombosis phenotypes. J Cell Molec Med 2021;25:9268-80.
13. Katz MH. Traditional Chinese medicine to prevent type 2 diabetes—a difficult path forward. JAMA Int Med 2024;184:736.
14. Xie C, Sun Q, Chen J, et al. Cu–Tremella fuciformis polysaccharide–based tumor microenvironment–responsive injectable gels for cuproptosis-based synergistic osteosarcoma therapy. Int J Biol Macromolec 2024;270:132029.
15. Li X, Su Q, Pan Y. Overcharged lipid metabolism in mechanisms of antitumor by Tremella fuciformis-derived polysaccharide. Int J Oncol 2022;62:11.
16. Wang J, Zhang S, Wang N, et al. *Tremella* polysaccharide has potential to retard wheat starch gel system retrogradation and mechanism research. Foods 2023; 12:3115.
17. Zhao X, Ma D, Yang B, et al. Research progress of T cell autophagy in autoimmune diseases. Front Immunol 2024;15:1425443.
18. Wang S, Chao X, Jiang X, et al. Loss of acinar cell VMP1 triggers spontaneous pancreatitis in mice. Autophagy 2022;18:1572-82.
19. Dikic I, Elazar Z. Mechanism and medical implications of mammalian autophagy. Nature Rev Molec Cell Biol 2018;19:349-64.
20. Kitada M, Koya D. Autophagy in metabolic disease and ageing. Nature Rev Endocrinol 2021;17: 647-61.
21. Ma Y, Jiao Z, Liu X, et al. Protective effect of adipose-derived stromal cell-secretome attenuate autophagy induced by liver ischemia–reperfusion and partial hepatectomy. Stem Cell Res Ther 2022; 13:427.
22. Scalabrin M, Engman V, Maccannell A, et al. Temporal analysis of skeletal muscle remodeling post hindlimb ischemia reveals intricate autophagy regulation. Am J Physiol Cell Physiol 2022;323: C1601-10.
23. Kamel R, El Morsy EM, Elsherbiny ME, Nour-Eldin M. Chrysin promotes angiogenesis in rat hindlimb ischemia: Impact on PI3K/Akt/mTOR signaling pathway and autophagy. Drug Develop Res 2022;83: 1226-37.
24. Surana R, Zheng H, Wang J, et al. Abstract A001: an open label, phase II trial of ERK inhibition alone and in combination with autophagy inhibition in patients with metastatic cancreatic cancer. Cancer Res 2024; 84:A001.
25. Stalnecker CA, Grover KR, Edwards AC, et al. Concurrent inhibition of IGF1R and ERK increases pancreatic cancer sensitivity to autophagy inhibitors. Cancer Research 2022;82:586-98.
26. Yu H, Lin Y, Zhong Y, et al. Impaired AT2 to AT1 cell transition in PM2. 5-induced mouse model of chronic obstructive pulmonary disease. Respir Res 2022; 23:70.
27. Ran J, Yin S, Issa R, et al. Key role of macrophages

in the progression of hepatic fibrosis. Hepatol Comm 2025;9:e0602.
28. Wang X, He B. Endothelial dysfunction: Molecular mechanisms and clinical implications. Med Comm 2024;5:e651.

Disclaimer

All claims expressed in this article are solely those of the authors and do not necessarily represent those of their affiliated organizations, or those of the publisher, the editors and the reviewers. Any product that may be evaluated in this article or claim that may be made by its manufacturer is not guaranteed or endorsed by the publisher.

Submitted: 29 August 2025.
Accepted: 24 September 2025.
Early access: 7 October 2025.